

Selective-precursor reducing route to cobalt nanocrystals and ferromagnetic property

Changlong Jiang*, Liyang Wang, Kunihiro Kuwabara

Department of Chemistry, National University of Singapore, 3 Science Drive 3, 117543 Singapore, Republic of Singapore

Received 12 May 2007; received in revised form 17 August 2007; accepted 16 September 2007

Available online 21 September 2007

Abstract

Cobalt nanocrystals were prepared by controlled chemical route at mild condition through selective-precursor reducing synthesis. Nanorod bundles and three-dimensional (3D) dendritic nanocrystal networks of Co were prepared by selecting different precursors. The samples were characterized by X-ray diffraction (XRD), scanning electron microscopy (SEM) and transmission electron microscopy (TEM) technologies. Field-emission scanning electron microscopy (FE-SEM), SEM, and TEM images indicate the nanorod bundles mainly consist of nanorods with the diameter of 70 nm. In 3D dendritic nanocrystal networks there are numerous secondary and sub-secondary branches were grown at right angles on each main stem. Room temperature magnetic measure of the Co samples demonstrates much enhanced ferromagnetic property, which might be attributed to their organization of specific shape. The possible formation mechanism of the cobalt nanocrystals with different morphologies was also discussed.

© 2007 Elsevier Inc. All rights reserved.

Keywords: Cobalt; Nanocrystals; Ferromagnetic

1. Introduction

The preparation of magnetic nanomaterials is of significant importance owing to their applications in ferrofluids, magnetic storage devices, magnetic refrigeration systems, contrast enhancement in magnetic resonance imaging, magnetic carriers for drug targeting, and catalysis [1–3]. There have been many efforts to synthesize magnetic nanomaterials with controllable shape and size due to their magnetic properties are dependent on the shape and size [4–7].

Among the three ferromagnetic metals (Fe, Co, and Ni), the nanomaterials of pure cobalt probably have special significance in both theory and technology because there exists uniaxial hexagonal close-packed (hcp or α -Co) structure besides face-centered cubic (fcc or β -Co) structure [8–10]. Many methods were applied to synthesize low-dimensional Co nanocrystallites, including decomposition

of organometallic precursors in the presence of a mixture of long-chain amines and oleic acid [11], electrochemical deposition [12], and chemical solution synthesis [13,14].

Since network structures fabricated with specific shape nanocrystals as building blocks can function both as devices and interconnections, they are expected to play a key role in the production of the next generation of nanoscale electric and optoelectronic devices [15–20]. However, the preparation of Co nanocrystal networks with specific morphology has not yet reported before. In this manuscript we report, for the first time, the synthesis of Co three-dimensional (3D) dendritic nanocrystal networks by a facile precursor reducing process, in which numerous secondary and sub-secondary branches were grown at right angles on each main stem. By selecting the precursor, we also have prepared Co nanorod bundles in similar condition. This synthesis route has demonstrated that it's possible to fabricate magnetic nanocrystals with different morphologies by a rational, facile solution progress, which might be applied to morphology-control synthesis of other inorganic materials with controllable structures.

*Corresponding author. Fax: +65 67791691.

E-mail address: chmjc@nus.edu.sg (C. Jiang).

2. Experimental section

All the reagents (analytical grade purity) were purchased from Sigma Aldrich Chemical and used without further purification.

2.1. Synthesis of three-dimensional (3D) dendritic nanocrystal networks

In a typical experiment, 0.01 mol $\text{CoCl}_2 \cdot 6\text{H}_2\text{O}$ and 0.01 mol Na_2CO_3 were dissolved in 20 ml deionized water, then added 0.05 mol $\text{NaH}_2\text{PO}_2 \cdot \text{H}_2\text{O}$ to above solution under continuous stirring for 5 min, the mixed solution was loaded into a 50 ml Teflon-lined stainless-steel autoclave, which was filled with distilled water up to 90% of the total volume, sealed and kept at 140°C for 72 h. The resulting product was filtered off, washed with absolute ethanol and distilled water for several times, finally dried in vacuum at 60°C for 4 h.

2.2. Synthesis of crystalline nanorod bundles

In a typical experiment, 0.01 mol $\text{CoCl}_2 \cdot 6\text{H}_2\text{O}$ and 0.025 mol NaOH were dissolved in 20 ml deionized water, then added 0.05 mol $\text{NaH}_2\text{PO}_2 \cdot \text{H}_2\text{O}$ to above solution under continuous stirring for 5 min, the mixed solution was loaded into a 50 ml Teflon-lined stainless-steel autoclave, which was filled with distilled water up to 90% of the total volume, sealed and kept at 140°C for 72 h. The resulting product was filtered off, washed with absolute ethanol and distilled water for several times, finally dried in vacuum at 60°C for 4 h.

2.3. Characterization

X-ray diffraction (XRD) pattern was determined using a Philips X'Pert PRO SUPER X-ray diffractometer equipped with graphite monochromatized $\text{CuK}\alpha$ radiation ($\lambda = 1.541874 \text{ \AA}$). Scanning electron microscopy (SEM) and field-emission scanning electron microscopy (FE-SEM) images were carried out with an X-650 scanning electron microanalyzer and a FE scanning electron microanalyzer (JEOL-6300F, 15 kV) respectively. Transmission electron microscopy (TEM) and high-resolution transmission electron microscopy (HRTEM) patterns were taken on a Hitachi Model H-800 and a JEOL-2010 TEM both with an accelerating voltage of 200 kV, respectively. The room temperature magnetic characterization of the sample was performed by a BHV-55 vibrating sample magnetometer.

3. Results and discussions

Fig. 1 shows the XRD patterns of the as-prepared samples. The peaks of diffraction from Fig. 1a (3D dendritic nanocrystal networks) could be indexed to hcp Co with cell constants $a = 2.511 \text{ \AA}$ and $c = 4.101 \text{ \AA}$, Fig. 1b is the pattern of the nanorod bundles with hcp cell

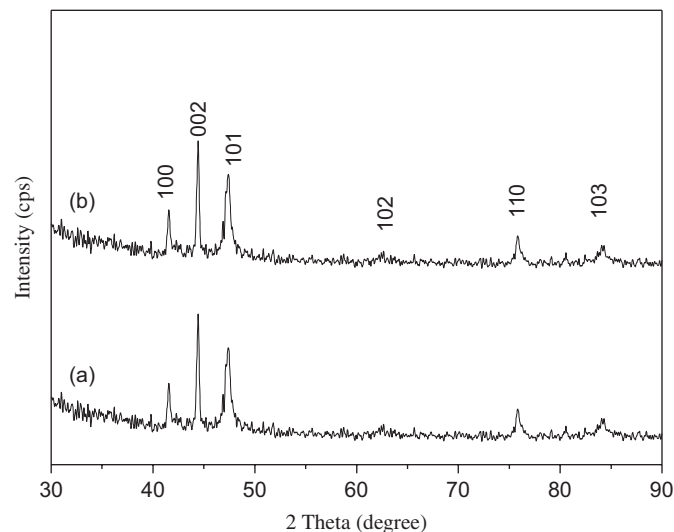


Fig. 1. XRD patterns of the samples: (a) 3D dendritic nanocrystal networks obtained in the presence of Na_2CO_3 at 140°C for 72 h, (b) nanorod bundles prepared with stirring in the presence of NaOH at 140°C for 72 h.

constants $a = 2.512 \text{ \AA}$ and $c = 4.102 \text{ \AA}$, both in good agreement with the reported data (JCPDS 01-1278, $a = 2.514 \text{ \AA}$, $c = 4.105 \text{ \AA}$). No impurities could be detected in the patterns, which imply pure hcp Co phase could be obtained under the current synthetic route.

Fig. 2a shows the panorama of the cobalt 3D networks of dendritic nanocrystal obtained in the presence of Na_2CO_3 at 140°C for 72 h in aqueous solution, in which the dendritic nanocrystal interconnected to form networks. A typical network structure is displayed in Fig. 2b, and numerous secondary and sub-secondary branches were grown at right angles on each main stem of the dendritic crystal, the main stem is $10 \mu\text{m}$ in length and some secondary branches have length of $1\text{--}5 \mu\text{m}$, all the branches have the diameters ranging from 50 to 100 nm. Fig. 2c demonstrates a single dendritic nanocrystal with many parallel secondary branches, from which some withes were also noticed grown at right angles; the main stem of the dendritic nanocrystal is above $10 \mu\text{m}$ long. The growth of the cobalt dendritic nanocrystal networks from the aqueous solution might be intriguing. To further elucidate the formation of the cobalt 3D networks, we studied the influence of several reaction parameters on the final sample. The addition of Na_2CO_3 , the reaction temperature and time are some of the parameters that determine the outcome of the crystallization. When performed the reaction without Na_2CO_3 but other parameters unchanged, the obtained sample only contains Co nanoparticles. While used hydrazine hydrate ($\text{N}_2\text{H}_4 \cdot \text{H}_2\text{O}$) as the reducing agent the obtained product is only nanoparticles. Fig. 2d is the product synthesized at 140°C for 12 h; some rod-like nanoparticles were noticed. When prolonged the reaction time to 24 h (Fig. 2e), the final sample consists of nanorods in diameter of 70 nm and some short dendritic structures, this is indicative of Ostwald ripening progress in the

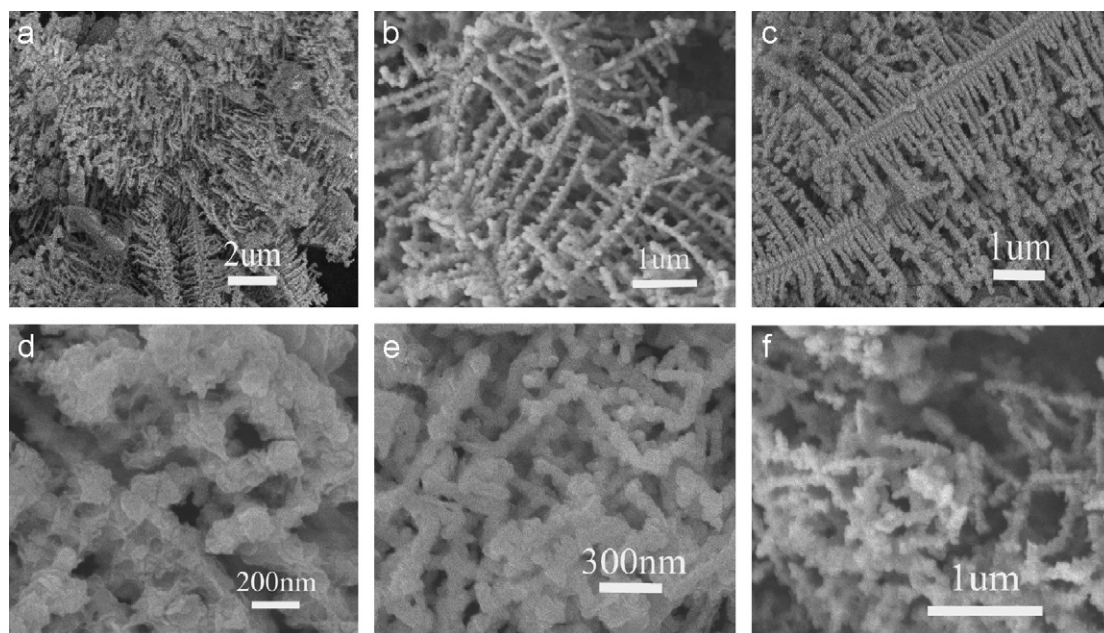


Fig. 2. FE-SEM images of the Co dendritic nanocrystal networks (a–c) synthesized at 140 °C for 72 h; Co samples obtained at 140 °C for 12 h (d), 24 h (e), and 48 h (f).

current synthesis. Fig. 2f is the product prepared at 140 °C for 48 h; the majority is a network composed of uncompleted dendritic structures. When reacted at 200 °C we only obtained nanoparticles with few nanorods (not shown) since the crystal growth rate is large in higher temperature.

The product was further characterized by TEM, selected area electron diffraction (SAED), and HRTEM techniques. Fig. 3a is the typical TEM pattern of the obtained Co dendritic nanocrystal networks; numerous secondary and sub-secondary branches of the dendritic nanocrystals were interconnected to form the network structures. The clear network structure was shown in Fig. 3b, in which many secondary and sub-secondary branches were interconnected at right angles to form the network structure, the diameter of the branches is about 50–70 nm. A single Co dendritic nanocrystal was presented in Fig. 3c; the dendritic nanocrystal structure has a main stem, which consisted of many secondary and sub-secondary branches in diameter of 50–70 nm. Fig. 3d demonstrated a single branch with the diameter of 70 nm, the corresponding SAED pattern (inserted Fig. 3d) could be indexed to hcp phase of Co and proved its single crystalline nature. An HRTEM image taken near the main stem of the dendritic nanocrystal is shown in Fig. 3e. As seen from this image, the dendritic nanocrystal is structurally uniform single crystalline, further structural analysis indicates the growth direction of the main stem of the dendritic crystal is parallel to the [100] crystalline orientation of Co.

When substituting NaOH for Na₂CO₃ under similar experiment condition another shape of Co nanocrystals was obtained. Fig. 4a shows the obtained Co sample at 140 °C for 72 h in the presence of NaOH, which displays nanorod bundles with the diameter of 0.5–1.5 and 3 μm

long, the nanorod bundles distribute randomly and consist of several up to a few tens nanorods. The high-resolution FE-SEM image of the nanorod bundles is presented in Fig. 4b; the nanorod bundles contain about 30 single nanorods with the diameter of 70 nm and length of 3 μm. To further elucidate the formation of the crystalline nanorod bundles, we studied the influence of several reaction parameters on the final sample. When synthesized at 140 °C for 24 h with stirring in the presence of NaOH, nanoparticles and few rod-like particles were noticed. When prolonged the reaction time to 48 h, the final sample consists of nanorods in diameter of 70 nm and some nanorod bundles. The diameter of the nanorod increased to 300 nm when the reaction temperature is 200 °C for 72 h with stirring in the presence of NaOH. Similar to the results of 3D dendritic nanocrystal networks the addition of NaOH, the reducing agents, the reaction temperature and time also influenced the final products.

The Co nanorod bundles were also characterized by TEM technique. A typical Co nanorod bundle is displayed in Fig. 4c; the bundle mainly contains about 20 nanorods in the diameter of 50–80 nm, some nanorods have tapering end. Fig. 4d is the typical TEM image of a single Co nanorod with the diameter of 70 nm; the corresponding electron diffraction (ED) is inserted in Fig. 4d, which could be indexed to hcp phase of Co. HRTEM pattern of the Co nanorod bundles is presented in Fig. 4e, the measured spacing of the crystallographic planes is 0.22 nm, which corresponds to the {100} lattice planes of pure hcp Co phase and indicates the nanorod bundles grow along the [100] axis.

Compared to previous reports on the cobalt nanorods, for example, Alivisatos et al. [21] prepared the cobalt

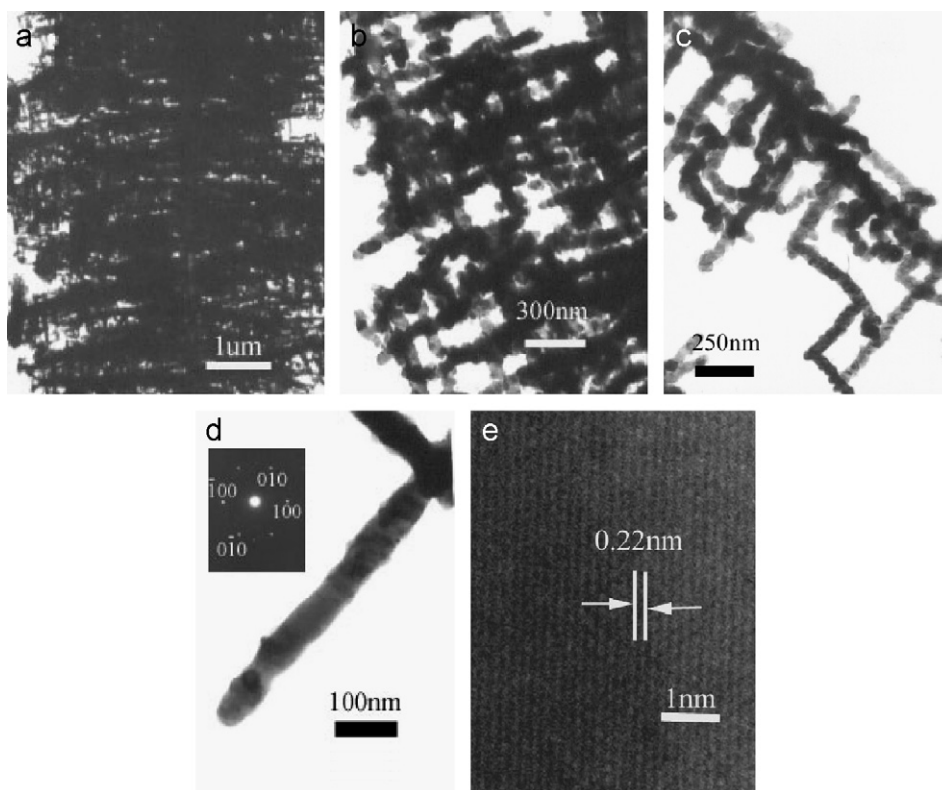


Fig. 3. TEM patterns of Co dendritic nanocrystal networks (a–c), a single branch and corresponding SAED image (d), HRTEM image of the Co sample (e).

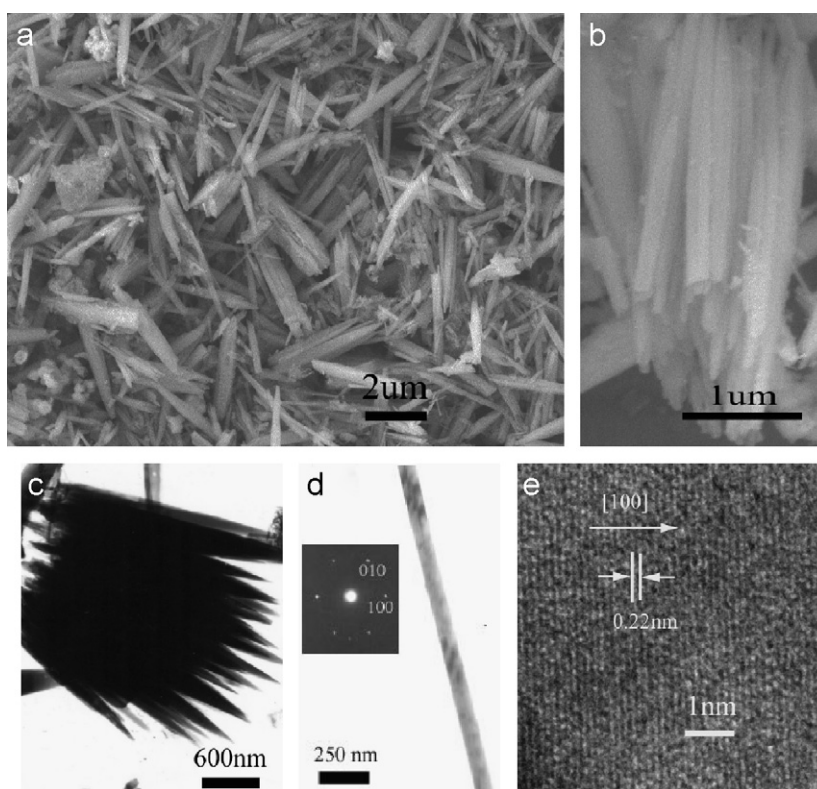
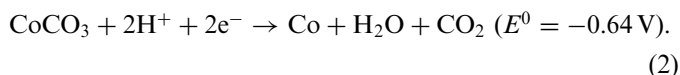
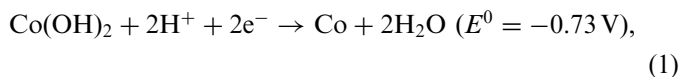


Fig. 4. FE-SEM (a, b) images of the Co nanorod bundles synthesized at 140 °C for 72 h in the presence of NaOH; TEM patterns of the sample synthesized at 140 °C for 72 h in the presence of NaOH: a typical nanorod bundle (c) and a single Co nanorod (d) (inserted in d: corresponding electron diffraction image), HRTEM pattern (e).

nanocrystals by injection of an organometallic precursor into a hot surfactant mixture under inert atmosphere, Chaudret et al. produced the cobalt nanorods through decomposition of organometallic precursors in the presence of a mixture of long-chain amines and oleic acid [6,11], the current synthesis adopted a simple chemical route without solvent, ligand or organic stabilizer. This implied that it's possible to fabricate metal nanostructures with special morphology via a rational, facile solution progress; the current synthesis process might be applied to the synthesis of other inorganic materials on the nanoscale.

Considering the experiment results, possible formation of the Co samples might be formed by a dissolution–recrystallization–reduction–growth process, which is similar to the solution-solid (SS) process [22,23]. At the early stage Co^{2+} aqueous solution reacting with Na_2CO_3 or NaOH resulted in CoCO_3 or Co(OH)_2 , which might be served as the precursor for the further growth of Co sample and sharply decreased the free Co^{2+} concentration in the solution. Milder than hydrazine hydrate, using $\text{NaH}_2\text{PO}_2 \cdot \text{H}_2\text{O}$ as the reducing agent could slow the generation of Co atoms from the solution. Therefore the quantity of the newly formed Co nanoparticles under current process was maintained at a low level, finally Co samples were obtained by the oriented attachment of the newly formed Co nanoparticles. In current synthesis the selective-precursor reducing route is very intriguing. The standard of the formal potential of the two reactions formulated as Eqs. (1) and (2):



From above analysis, the reaction tendency of (1) is larger than that of (2), which implies the reducing reaction from Co(OH)_2 to Co will be faster than that from CoCO_3 to Co. The difference in the reaction tendency results in change of the crystal growth rate. When CoCO_3 served as the precursor the system was dominated by lower reaction potential, thus the nucleation of Co nanoparticles was very slow, which provided a favorable condition for the growth of the dendritic nanocrystal networks of Co. While in the case Co(OH)_2 , the progress will be faster than that of CoCO_3 and the nucleation of Co nanoparticles is also high, which resulted in the final formation of nanorod bundles. Another possible attribution is the magnetic energy can help the generation of the final Co samples with special shapes. However, the special formation progress of the nanorod bundles is not yet clear and warrants further investigation, the related study is still under way.

3.1. Magnetic characterization of the samples

The magnetic properties of nanomaterials have been believed to be highly dependent on the sample shape,

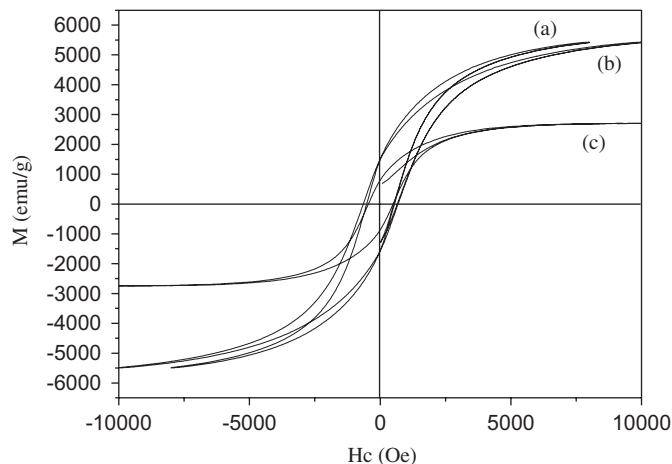


Fig. 5. Room-temperature hysteresis loops: (a) nanorod bundles prepared at 140°C for 72 h with stirring in the presence of NaOH , (b) three-dimensional dendritic nanocrystal networks obtained in the presence of Na_2CO_3 at 140°C for 72 h, and (c) nanoparticles fabricated at 140°C for 72 h.

crystallinity, magnetization direction, and so on. Thus, a remarkably enhanced ferromagnetic property of the as-prepared Co samples, comparable to that of Co nanoparticles, should be supposed. The hysteresis loops of the Co crystalline nanorod bundles (Fig. 5a) and 3D dendritic nanocrystal networks (Fig. 5b) measured at room temperature show a ferromagnetic behavior with coercivity (H_c) value of ca. 695.1 and 597.5 Oe, respectively. From a magnetic point view, the two Co samples with nanorod bundles and 3D dendritic nanocrystal networks shapes display an effective anisotropy as a consequence of both their shape and crystalline structure. Compared to the H_c value of bulk Co (a few tens of oersteds) [24] and that of Co nanoparticles (ca. 245.7 Oe) (see Fig. 5c), the obtained Co samples exhibit enhanced coercivity, which might be attributed to their organization of specific nanostructures, the sample with high crystalline anisotropy or shape anisotropy often possess high coercivity [25,26].

4. Conclusions

In summary, we have presented the selective-precursor reducing synthesis of Co nanorod bundles and 3D dendritic nanocrystal networks in aqueous solution at mild condition. Room temperature magnetic measure of the Co samples demonstrates much enhanced ferromagnetic property, which might be attributed to their organization of specific shape. Several factors that influenced the final products were also discussed. This synthesis progress could be extended to fabricate other metal nanocrystallines with controllable morphology.

Acknowledgment

Financial support from the National University of Singapore is gratefully acknowledged.

References

- [1] S. Sun, C.B. Murray, D. Weller, L. Folks, A. Moser, *Science* 287 (2000) 1989.
- [2] F. Mikulec, M. Kuno, M. Bennati, D. Hall, R. Griffin, M. Bawendi, *J. Am. Chem. Soc.* 122 (2000) 2532.
- [3] S. Kim, S. Son, S. Lee, T. Hyeon, Y. Chung, *Chem. Commun.* (2001) 2212.
- [4] S. Sun, H. Zeng, *J. Am. Chem. Soc.* 124 (2002) 8204.
- [5] F. Dumestre, B. Chaudret, C. Amiens, P. Renaud, P. Fejes, *Science* 303 (2004) 821.
- [6] F. Dumestre, B. Chaudret, C. Amiens, M. Respaud, P. Fejes, P. Renaud, P. Zurcher, *Angew. Chem. Int. Ed.* 42 (2003) 5213.
- [7] J. Park, B. Koo, Y. Hwang, C. Bae, K. An, J. Park, H. Park, T. Hyeon, *Angew. Chem. Int. Ed.* 43 (2004) 2282.
- [8] H. Gleiter, *Prog. Mater. Sci.* 89 (1989) 223.
- [9] J. Chen, C. Sorensen, K. Klabunde, C. Hadjipanayis, *Phys. Rev. B* 51 (1995) 11527.
- [10] W. Gong, H. Li, Z. Zhao, J. Chen, *J. Appl. Phys.* 69 (1991) 5119.
- [11] F. Dumestre, B. Chaudret, C. Amiens, M. Fromen, M. Casanove, P. Renaud, P. Zurcher, *Angew. Chem. Int. Ed.* 41 (2002) 4286.
- [12] H. Cao, Z. Xu, H. Sang, D. Sheng, C. Tie, *Adv. Mater.* 13 (2001) 121.
- [13] S. Sun, C. Murray, *J. Appl. Phys.* 85 (1999) 4325.
- [14] Y. Sun, H. Rollins, R. Guduru, *Chem. Mater.* 11 (1999) 7.
- [15] Z. Wang, Z. Pan, *Adv. Mater.* 14 (2002) 1029.
- [16] M. Diehl, S. Yaliraki, R. Beckman, M. James, R. Heath, *Angew. Chem. Int. Ed.* 41 (2002) 353.
- [17] Y. Huang, X. Duan, Y. Cui, L. Lauthon, K. Kim, C. Lieber, *Science* 294 (2001) 1313.
- [18] Y. Huang, X. Duan, Q. Wei, C. Lieber, *Science* 291 (2001) 630.
- [19] Y. Cui, C. Lieber, *Science* 291 (2001) 851.
- [20] N. Kovtyukhova, T. Mallouk, *Chem. Eur. J.* 8 (2002) 4355.
- [21] V. Puentes, D. Zanchet, C. Erdonmez, A. Alivisatos, *J. Am. Chem. Soc.* 124 (2003) 12874.
- [22] A. Xu, Y. Fang, L. You, H. Liu, *J. Am. Chem. Soc.* 125 (2003) 1494.
- [23] J. Wang, L. Gao, *J. Mater. Chem.* 13 (2003) 2551.
- [24] V. Puentes, K. Krishnan, A. Alivisatos, *Science* 291 (2001) 2115.
- [25] D. Dinega, M. Bawendi, *Angew. Chem. Int. Ed.* 38 (1999) 1788.
- [26] S. Park, S. Kim, S.Y. Lee, Z.G. Khim, K. Char, T. Hyeon, *J. Am. Chem. Soc.* 122 (2000) 8581.